Journal of Fluorescence
https://doi.org/10.1007/s10895-024-03692-y

RESEARCH

Synthesis and Application of 1,8-Naphthalimide Derivatives Fluorescent Probe for Sequential Recognition of Cu^{2+} and $H_2PO_4^-$

Shukui Pang[1] · Yanchao Yu[1] · Wenju Wu[1] · Mianyuan Wu[2] · Jun You[1] · Canyao Wu[1] · Panru Zu[1]

Received: 28 February 2024 / Accepted: 26 March 2024

Abstract
A naphthalimide Schiff base fluorescent probe (BSS) was designed and synthesized from 4-bromo-1,8-naphthalic anhydride, and its structure was characterized by ^{1}HNMR, ^{13}CNMR, FTIR, and MS. Fluorescence emission spectra showed that probe BSS could realize the "turn-off" detection of Cu^{2+} in acetonitrile solution, detection process with strong specificity and excellent anti-interference of other metal ions. In the fluorescence titration experiments, fluorescence intensity of BSS showed a good linear relationship with the Cu^{2+} concentration (0–10 μmol/L), and the detection limit was up to 7.0×10^{-8} mol/L. Meanwhile, BSS and Cu^{2+} could form a 1:1 complex (BSS-Cu^{2+}) during the reaction process. Under the same detection conditions, complex BSS-Cu^{2+} had specific fluorescence recovery properties for $H_2PO_4^-$ and the whole process was not only fast (6 s) but also free of interference from other anions, with a detection limit was as low as 5.7×10^{-8} mol/L. In addition, complex BSS-Cu^{2+} could be successfully applied to the detection of $H_2PO_4^-$ in actual water samples, which with excellent application prospects.

Keywords Naphthalimide Schiff base · Fluorescent probe · Cu^{2+} · $H_2PO_4^-$ · Relay detection

Introduction

Copper is one of the essential trace elements for living organisms and a redox-active nutrient required for life activities, playing an important role in many key physiological and pathological processes. An imbalance of copper ion levels in an organism or cell could lead to a variety of serious diseases such as cancer [1, 2], cardiovascular disease [3], Alzheimer's disease (AD) [4], obesity and diabetes [5, 6]. However, there are many reasons for the imbalance of copper in organisms, among which environmental pollution is an important factor. Due to the extensive use of copper in electric power and electroplating industries, release of excess copper ions into environment has caused serious environmental pollution [7, 8] and has entered the organisms through food chain enrichment. Therefore, it is essential to strengthen the monitoring of copper ions in environment to eliminate the excessive intake of copper ions at the source.

Like copper ions, inorganic phosphates are an essential class of anions associated with life activities and play important roles in genetic information storage, gene regulation, and muscle contraction [9]. Dihydrogen phosphate ($H_2PO_4^-$) is one of the more important parts of it, which not only plays an important role in signal transduction and energy storage in living systems [10, 11], but also is in a dominant equilibrium with other two basic anions (HPO_4^{2-} and PO_4^{3-}), which plays a huge role in maintaining pH stability in the body. However, the occurrence of some diseases is related to the level of phosphorus in the body, such as increased levels of phosphorus salts in the blood could trigger hyperphosphatemia, which seriously affects human health [12, 13]. In addition, the impact of phosphate on the environment and ecology is also obvious to all, the eutrophication of water bodies caused by excessive phosphate [14–17] brings many inconveniences to people's production

✉ Yanchao Yu
yychao136@163.com

✉ Wenju Wu
wuwenju1017@163.com

[1] Key Laboratory of Green Chemical Engineering and Technology of College of Heilongjiang Province, School of Materials Science and Chemical Engineering, Harbin University of Science and Technology, Harbin 150080, P. R. China

[2] Institute of Petrochemistry, Heilongjiang Academy of Sciences, Harbin 150040, P. R. China

Published online: 13 April 2024

and life, therefore, the detection of phosphate ions is also an aspect of environmental management focused on.

Common analytical methods such as chromatography, spectrophotometry [18], enzyme biosensors [19], mass spectrometry, ICP-AES, and electrochemical methods [20–22] could be used for the detection of Cu^{2+} or $H_2PO_4^-$. Although these methods could achieve selective and sensitive detection of two ions, some of them are time-consuming, complicated operation, require expensive equipment, and these shortcomings limit the application of methods in practice. Compared with the above methods, fluorescence detection has been widely used to identify and detect various ions in environmental systems because of the advantages of easy operation, strong visualization, in vivo and on-site detection, and low requirements for operators [23–26]. Up to date, compared with the previous single-target response fluorescent probes, single-molecule fluorescent systems which could capable of simultaneous determination of multiple analytes have attracted more attention in recent years because of their simplicity, low cost, and high efficiency [27–31].

1,8-Naphthimide is one of the most commonly used fluorophores in the synthesis of fluorescent probes. Its derivatives not only have high quantum yield and good photostability but also are widely used in the field of fluorescent probe preparation by adjusting the substituents attached to the nitrogen atom of the 1,8-naphthoimide fragment and the 4,5 or 3,4 position of the naphthalene ring portion, which results in good compatibility and high selectivity [32–35]. Therefore, in this paper, by introducing ethanolamine as an electron-donating group at the 4-position of the naphthalene ring, through the condensation reaction between nitrogen atom of the 1,8-naphthoimide fragment and 5-bromosalicylaldehyde, a Schiff base fluorescent probe (BSS) was designed and synthesized using naphthylimide as the fluorescent group and hydroxyl, carbonyl, and imine groups as the sites of action. Fluorescence of BSS was quenched upon complexation with Cu^{2+}; After continuing to add $H_2PO_4^-$, due to its strong complexation with Cu^{2+}, which could be displaced to make the probe BSS in free state, and the fluorescence was recovered again. The whole tandem detection process was very fast. As a result, probe BSS could realize "ON-OFF-ON" specific fluorescence sequential recognition of Cu^{2+} and $H_2PO_4^-$ under the same test conditions. In addition, complex BSS-Cu^{2+} could also be applied to the qualitative and quantitative detection of $H_2PO_4^-$ in real water samples, which provided a new way to detect $H_2PO_4^-$ in the environment.

Experimental

Materials and Instruments

4-bromo-1,8-naphthalic anhydride, 5-bromosalicylaldehyde, ethanolamine, Anergy Chemical Reagent Company; Hydrazine hydrate (80w%), Tianjin Damao Chemical Reagent Factory; Reagents used in experiments were commercially available in analytical purity; Water used in the labs was secondary distilled water.

AV-300 MHz Nuclear Magnetic Resonance Spectrometer, Bruker, Germany; F-4500 Fluorescence Spectrometer, Hitachi High-Technologies, Japan; UV-2450 Ultraviolet Spectrophotometer, Shimadzu, Japan; Nicolet 370 Fourier Transform Infrared (FTIR) Spectrometer, Thermo Fisher Scientific, USA; SolariX 70 FT Mass Spectrometer, Bruker, Germany.

Synthesis and Structure Characterization of Probe BSS

Synthesis route of probe BSS was displayed in Scheme 1. In a 100 mL three-necked flask, a mixture of 4-bromo-1, 8-naphthalic anhydride (1.26 g, 4.5 mmol), 80w% hydrazine hydrate (0.34 g, 5.5 mmol), and anhydrous ethanol was added, refluxed and stirred until the reaction was completed. The progress of the reaction was tracked through thin-layer chromatography (TLC). After the reaction solution was cooled to room temperature, the precipitate was filtered and washed with ethyl acetate to give 1.10 g of earthy yellow

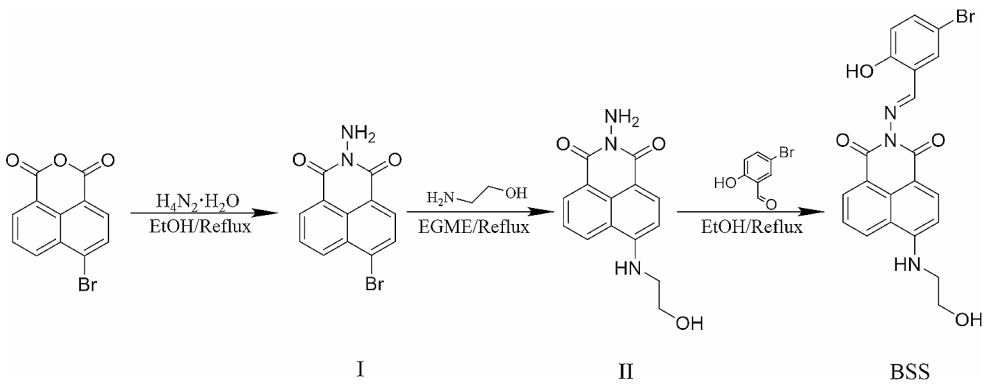

Scheme 1 Synthesis route of probe BSS

solid (Intermediate I) in 83.3% yield. ^{1}H NMR (300 MHz, DMSO-d_6) δ 8.53 (dd, J = 14.8, 7.7 Hz, 2 H), 8.31 (d, J = 7.9 Hz, 1H), 8.19 (d, J = 7.8 Hz, 1H), 7.97 (t, J = 7.9 Hz, 1H), 5.79 (s, 2 H) ppm, (Fig. S1).

In a 100 mL three-necked flask, Intermediate I (0.30 g, 1.03 mmol), ethanolamine (0.13 g, 2.16 mmol), and ethylene glycol methyl ether 20 mL were added. Mixture was heated and stirred until the reaction was completed. The progress of the reaction was tracked through thin-layer chromatography (TLC). After the reaction cooled to room temperature, spin evaporated off most of the solvent and added a small amount of water to dissolve. At this time the precipitation of orange solid, filtration, drying, solid 0.17 g (Intermediate II), yield 61.4%. ^{1}H NMR (300 MHz, DMSO- d_6) δ 8.71 (d, J = 7.6 Hz, 1H), 8.45 (d, J = 6.4 Hz, 1H), 8.26 (d, J = 8.5 Hz, 1H), 7.82 (t, J = 5.7 Hz, 1H), 7.69 (t, J = 6.0 Hz, 1H), 6.82 (d, J = 8.7 Hz, 1H), 5.73 (s, 2 H), 4.89 (t, J = 5.6 Hz, 1H), 3.69 (q, J = 5.7 Hz, 2 H), 3.47 (q, J = 6.0 Hz, 2 H) ppm, (Fig. S2). ^{13}C NMR (75 MHz, DMSO-d_6) δ 160.65, 160.50, 151.65, 134.79, 131.03, 129.11, 128.38, 124.69, 121.79, 120.65, 107.37, 104.44, 59.24, 46.04 ppm, (Fig. S3). FTIR(KBr): 3329, 2923, 2853, 1686, 1632, 1589, 1449, 1396, 1370, 1260, 1242, 1130, 1066, 956, 893, 768, 582 cm^{-1}, (Fig. S4).

In a 25 mL three-necked flask, Intermediate II (0.05 g, 0.185 mmol), 5-bromosalicylaldehyde (0.04 g, 0.20 mmol), and anhydrous ethanol were added and refluxed. The progress of the reaction was tracked through thin-layer chromatography (TLC). After the reaction was completed and cooled to room temperature, solid was precipitated and dried to obtain yellow fluorescent probe BSS (0.065 g) in 77.3% yield. ^{1}H NMR (300 MHz, DMSO-d_6) δ 11.29 (s, 1H), 8.97 (s, 1H), 8.76 (d, J = 7.7 Hz, 1H), 8.49 (d, J = 6.4 Hz, 1H), 8.30 (d, J = 8.6 Hz, 1H), 7.98 (d, J = 2.6 Hz, 1H), 7.89 (t, J = 5.3 Hz, 1H), 7.73 (dd, J = 8.3, 7.5 Hz, 1H), 7.61 (dd, J = 8.8, 2.6 Hz, 1H), 7.00 (d, J = 8.9 Hz, 1H), 6.87 (d, J = 8.7 Hz, 1H), 4.91 (t, J = 5.6 Hz, 1H), 3.72 (q, J = 5.7 Hz, 2 H), 3.50 (q, J = 5.8 Hz, 2 H) ppm, (Fig. S5). ^{13}CNMR (75 MHz, DMSO-d_6): δ 167.21, 161.12, 160.49, 158.28, 151.8, 136.55, 135.28, 131.89, 131.65, 129.51, 129.44, 124.83, 122.34, 120.69, 120.52, 119.63, 110.97, 107.56, 104.66, 59.26, 46.06 ppm, (Fig. S6). FTIR(KBr): 3439, 3389, 2922, 1676, 1647, 1619, 1586, 1475, 1357, 1276, 1154, 1079, 769 cm^{-1}, (Fig. S7). ESI-MS (m/z) calculated $[BSS + H]^+ = 454.0324$, found 454.0404, (Fig. S8).

Spectroscopic Measurements

Solutions of 16 metal ions (Cu^{2+}, Zn^{2+}, Ag^{+}, Ca^{2+}, Cr^{3+}, K^{+}, Al^{3+}, Fe^{3+}, Mg^{2+}, Pb^{2+}, Na^{+}, Cs^{2+}, Li^{+}, Cd^{2+}, Hg^{2+}, Bi^{2+}) and 17 anions (SO_3^{2-}, $S_2O_3^{2-}$, SO_4^{2-}, HSO_4^{-}, F^{-}, $H_2PO_4^{-}$, HPO_4^{2-}, PO_4^{3-}, NO_3^{-}, Br^{-}, I^{-}, HCO_3^{-}, CO_3^{2-}, Cl-, CH_3COO^{-}, $Cr_2O_7^{2-}$, $P_2O_7^{4-}$) were prepared at a concentration of 10 mmol/L using secondary distilled water as solvent. Probe BSS was dissolved in acetonitrile to formulate master mix at a concentration of 10 mmol/L, and prior to spectral measurement, master mix was diluted to 10 μmol/L with acetonitrile solution. In the solution of BSS, 1.0 eq. Cu^{2+} was added to obtain complex BSS-Cu^{2+} solution. All fluorescence tests were performed at room temperature with $\lambda_{ex} = 461$ nm, $\lambda_{em} = 541$ nm, and the slit widths were all 5 nm.

Actual Water Samples Measurement

Actual water samples were taken from tap water and Songhua River. Both samples were centrifuged at 12,000 r/min for 10 min and filtered through 0.45 μm membrane twice. Then 4 μmol/L, 8 μmol/L, 12 μmol/L, and 16 μmol/L potassium dihydrogen phosphate solutions were prepared, and spectral measurements were made under above test conditions.

Results and Discussion

Selectivity of Probe BSS for Cu^{2+}

Aqueous solutions of different metal ions were added to probe BSS, and fluorescence spectra were measured under 461 nm, results as shown in Fig. 1a. As the addition of Cu^{2+}, fluorescence intensity of BSS was quenched almost completely, and under 365 nm, yellow-green fluorescence of the probe was visible disappeared; Except for Mg^{2+} and Zn^{2+}, which caused a slight decrease of fluorescence intensity, other metal ions did not cause significant changes in the fluorescence intensity of probe BSS. In addition, UV spectra of BSS with different metal ions were examined, as shown in Fig. 1b. UV absorption peak of BSS appeared near 430 nm, with addition of Cu^{2+}, the peak was obviously red-shifted to the vicinity of 465 nm, and the color could be seen changed from light green to yellow, while other metal ions hardly affected the UV spectrum. Changes of fluorescence and UV spectral indicated that BSS could realize the specific recognition of Cu^{2+}, and the color changes also indicated the method had advantages of good visualization and easy operation compared with other detection methods.

Anti-Interference of Probe BSS for Cu^{2+}

Recognition performance of probe BSS for Cu^{2+} was investigated when different metal ions coexisted. As shown in Fig. 2, when various interfering metal ions were present in detection system, copper ions also could lead to a fluorescence quenching effect, which indicated that BSS had a

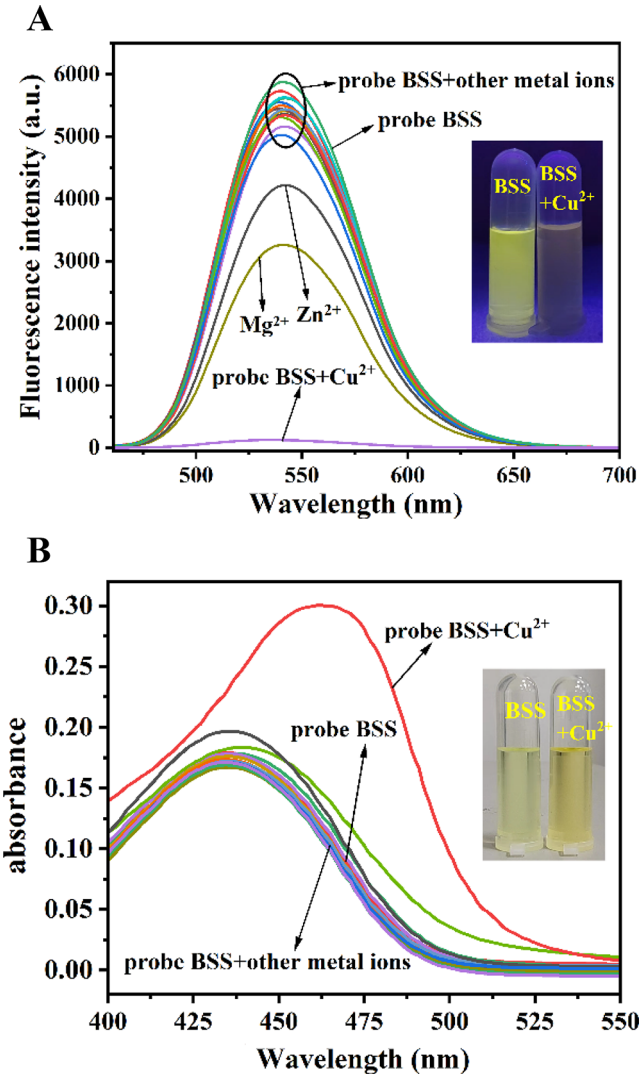

Fig. 1 (**a**) Fluorescence spectra of probe BSS (10 μmol/L) interacted with metal ions. Inset in **a** showed fluorescence change as addition of Cu^{2+} to BSS (10 μmol/L) under 365 nm. (**b**) UV spectrum of probe BSS (10 μmol/L) interacted with metal ions. Inset in **b** showed color change as addition of Cu^{2+} to BSS (10 μmol/L) under the sun lamp

well-developed immunity to interferences in the detection of Cu^{2+}. The reason may be the hydroxyl, carbonyl oxygen, and nitrogen atoms in BSS had a more stronger complexation ability with Cu^{2+}, which could generate the complex BSS-Cu^{2+} and lead to fluorescence quenching.

Sensitivity of Probe BSS for Cu^{2+}

To further investigate the sensitivity of BSS for Cu^{2+}, fluorescence titration experiments were performed. As shown in Fig. 3a, fluorescence intensity of BSS at 541 nm gradually decreased with gradual increase of Cu^{2+} concentration, as the concentration exceeded 12 μmol/L, fluorescence intensity no longer changed. When the concentration of copper

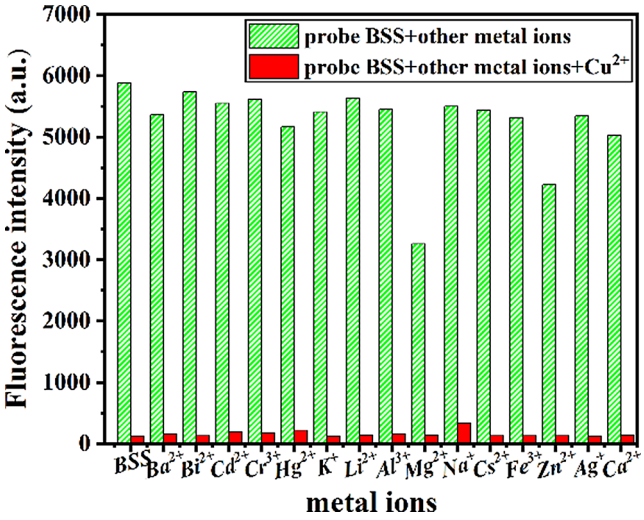

Fig. 2 Effect of coexisting metal ions on the recognition of Cu^{2+} by probe BSS (10 μmol/L)

ions was in the range of 1 ~ 10 μmol/L, fluorescence intensity showed a well-linear relationship with Cu^{2+} concentration (Fig. 3b), the linear regression equation was obtained as y=-464.85x + 5925.59 with $R^2 = 0.996$. Based on the formula LOD = 3σ/k (where σ is the standard deviation of fluorescence intensity and k is the slope of the linear regression equation), the detection limit of Cu^{2+} was calculated to be 7.0×10^{-8} mol/L, which far below the maximum limit of 2 ppm (30 μmol/L) recommended by the World Health Organization (WHO) for copper in drinking water [36]. Compared with other probe of Cu^{2+} [23, 27, 28, 31], probe BSS had an advantage in the detection limit of copper ions, which could realize trace detection of Cu^{2+} with high sensitivity.

Action Mode of Probe BSS with Cu^{2+}

In order to determine the ratio of probe to copper ions, a Job's plot curve was derived from data fitting as shown in Fig. 4a. It could be seen that fluorescence intensity inflected at a Cu^{2+} molar fraction of about 0.51, which indicated that the complexation ratio of BSS to Cu^{2+} was 1:1. Complexes BSS-Cu^{2+} was prepared and analyzed by mass spectrometry data, the result was shown in Fig. 4b. The $[BSS + Cu^{2+} + H]^+$ ion peak at m/z = 515.9025 in the figure agreed with the theoretical value of 515.9524, this data further demonstrated that the probe acted in a 1:1 ratio with copper ions.

In addition, complex BSS-Cu^{2+} IR spectra was measured and compared with probe BSS, results were shown in Fig. 5. In the spectra of probe, characteristic peaks of hydroxyl, carbonyl and imine bond appeared at 3439,1676 and 1619 cm^{-1} respectively; As complex formation, hydroxyl peak disappeared, carbonyl and imine bond shifted to 1670 and 1603 cm^{-1} respectively. These changes indicated that

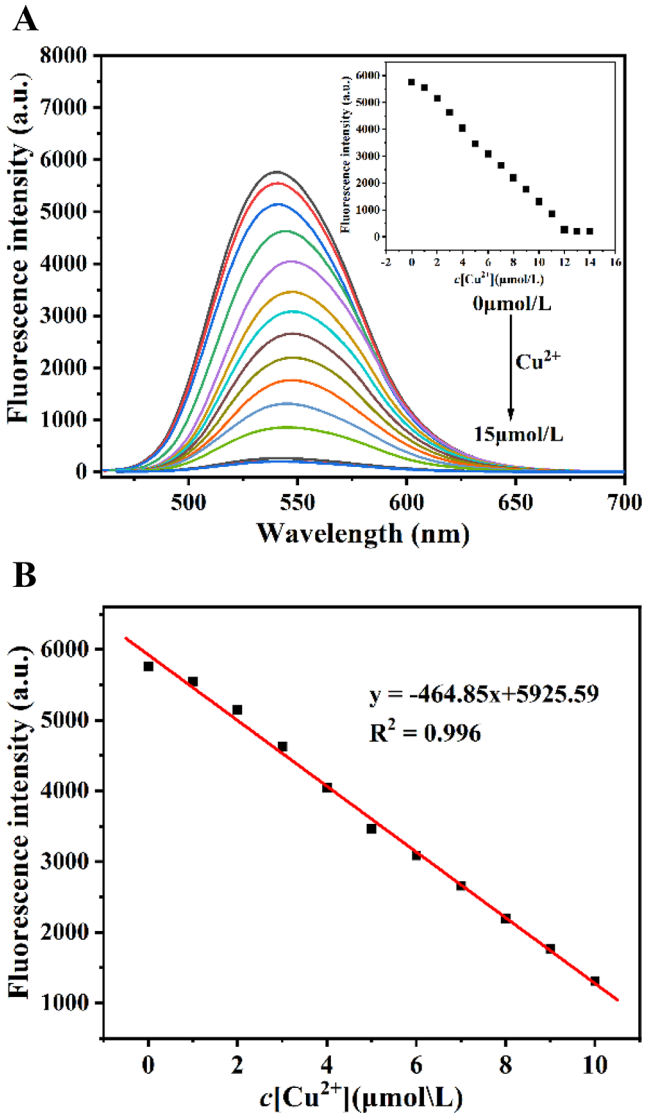

Fig. 3 (**a**) Fluorescence spectra and titration curves (as Inset showed) of probe BSS (10 μmol/L) at 541 nm with different Cu^{2+} (0–15 μM) concentrations. (**b**) Linearity between fluorescence intensity of probe BSS and Cu^{2+} (0–10 μM) concentration

hydroxyl, carbonyl, and imine bonds in the structure of BSS had been involved in the complexation of copper ions.

Selectivity of Complex BSS-Cu^{2+} for H_2PO_4

To a solution of complex BSS-Cu^{2+}, aqueous solution of SO_3^{2-}, $S_2O_3^{2-}$, SO_4^{2-}, HSO_4^-, F^-, $H_2PO_4^-$, HPO_4^{2-}, PO_4^{3-}, NO_3^-, Br^-, I^-, HCO_3^-, CO_3^{2-}, Cl^-, CH_3COO^-, $Cr_2O_7^{2-}$, $P_2O_7^{4-}$ was added separately, and fluorescence spectra were determined sequentially. As shown in Fig. 6a, with addition of $H_2PO_4^-$, the system showed an obvious fluorescence recovery, and the recovery rate reached 98.4%, at the same time, yellow-green fluorescence was restored under 365 nm. Although there was a slight fluorescence enhancement by HPO_4^{2-} and I^-, the effect was almost negligible compared to fluorescence restoration by $H_2PO_4^-$. Other than that, other anions did not cause significant fluorescence changes. This indicated that complex BSS-Cu^{2+} had a good selectivity for $H_2PO_4^-$. In addition, as shown in Fig. 6b, absorption peak of complex BSS-Cu^{2+} appeared at 465 nm; As addition of $H_2PO_4^-$, absorption peak was blue-shifted to 433 nm which basically overlapped with the absorption peak of BSS and the color changed back to light green, which indicated that $H_2PO_4^-$ could replace copper ions of BSS-Cu^{2+} and make BSS to be free. Other anions did not cause a shift in the absorption peak, which suggested that the specific recognition of $H_2PO_4^-$ could be achieved by BSS-Cu^{2+} with a naked eye.

Anti-Interference of Complex BSS-Cu^{2+} for H_2PO_4

Anti-interference properties of BSS-Cu^{2+} recognizing $H_2PO_4^-$ in the presence of coexisting anions were examined and results were shown in Fig. 7. Even with the coexistence of various anions, fluorescence intensity of system undergoes significant enhancement with the addition of $H_2PO_4^-$, and could be recovered to the vicinity of probe BSS, which indicated that complex BSS-Cu^{2+} had a very good anti-interference property for the recognition of $H_2PO_4^-$.

Sensitivity of Complex BSS-Cu^{2+} for H_2PO_4

Fluorescence titration experiments were performed to further investigate the detection sensitivity of BSS-Cu^{2+} to $H_2PO_4^-$. As shown in Fig. 8a, fluorescence intensity of BSS-Cu^{2+} at 541 nm gradually increased with the increasing of $H_2PO_4^-$ concentration; As concentration exceeded 20 μmol/L, fluorescence intensity no longer changed. Moreover, in the concentration range of 0 ~ 19 μmol/L, fluorescence intensity showed a good linear relationship with $H_2PO_4^-$ concentration (Fig. 8b), and a linear regression equation was fitted as $y = 308.57x + 139.50$ with $R^2 = 0.993$. Subsequently, the detection limit of $H_2PO_4^-$ was calculated to be 5.7×10^{-8} mol/L according to the formula $LOD = 3\sigma/k$, and compared with other probe [24, 29, 30], complex BSS-Cu^{2+} had advantage in the trace detection of $H_2PO_4^-$ with high sensitivity.

Recognition Mechanism between BSS-Cu^{2+} and H_2PO_4

In addition, Job's plot curve (Fig. 9a) was derived from data fitting, and it could be seen that molar fraction of $H_2PO_4^-$ showed an inflection point at approximately 0.67, which indicated a 1:2 ratio of the action between BSS-Cu^{2+} and $H_2PO_4^-$. Reversibility experiments with alternate addition

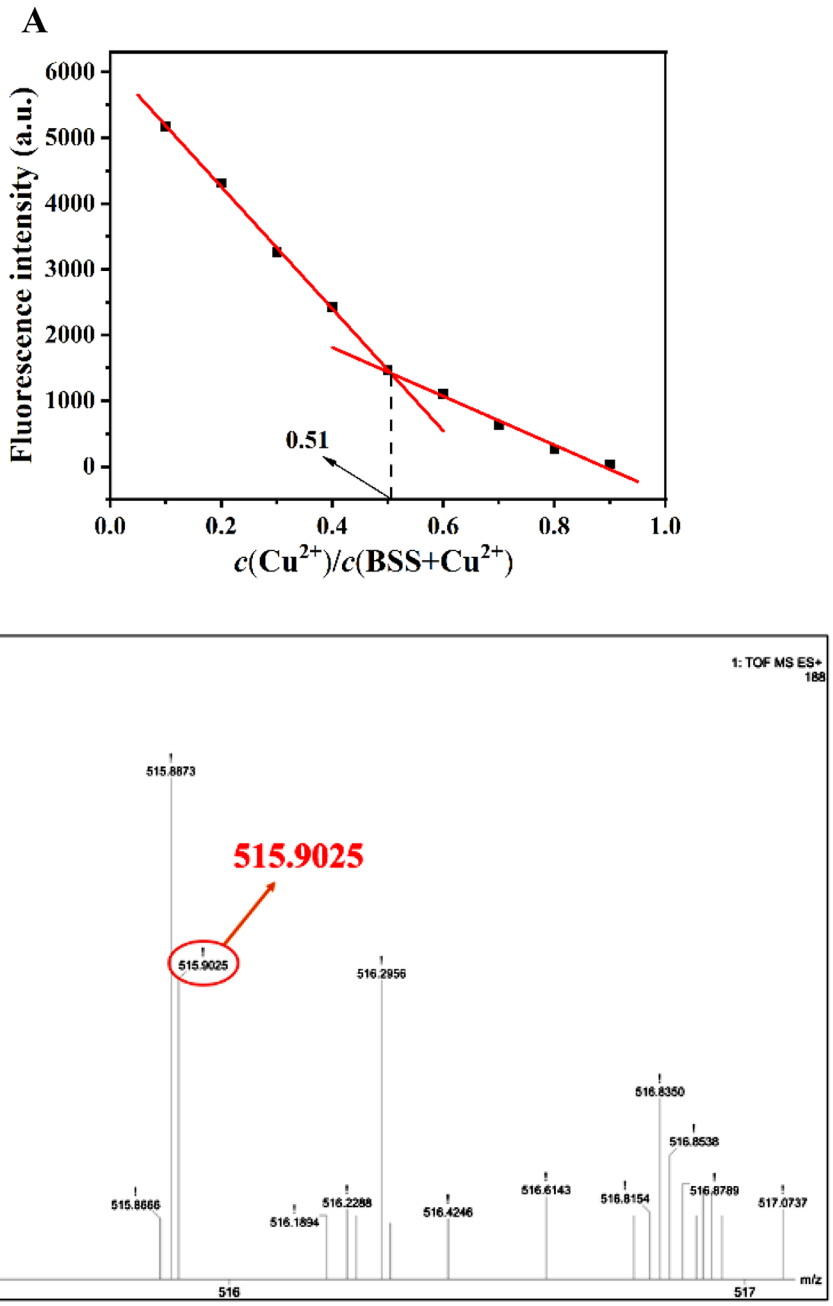

Fig. 4 (**a**) Job's plot of probe BSS with Cu^{2+}, in which $c(BSS + Cu^{2+}) = 10$ μmol/L. (**b**) Mass spectra of complex BSS-Cu^{2+}

of Cu^{2+} and $H_2PO_4^-$ to the probe BSS solution were carried out (Fig. 9b), which showed that fluorescence intensity of BSS was not significantly attenuated for more than 5 cycles, indicating the stable nature of BSS. The detection mechanism that $H_2PO_4^-$ could capture Cu^{2+} of complex BSS-Cu^{2+} to free BSS was also further verified. Based on experimental data, the mechanism of probe BSS to recognize Cu^{2+} and $H_2PO_4^-$ continuously was hypothesized as shown in Fig. 10.

Effect of Time on Probe BSS

Finally, response time of probe BSS to Cu^{2+} and BSS-Cu^{2+} to $H_2PO_4^-$ were investigated respectively, the findings were depicted in Fig. 11. Within 2 s of Cu^{2+} being added, the probe's fluorescence rapidly declined. As time elapsed, fluorescence intensity reached a stable point at the 6th second when the fluorescence of probe BSS was suppressed. Similarly, fluorescence intensity reached its maximum at the 6th s after addition of $H_2PO_4^-$ to complex BSS-Cu^{2+}, which basically recovered to the same fluorescence intensity as that of BSS. Probe BSS and complex BSS-Cu^{2+} had shorter

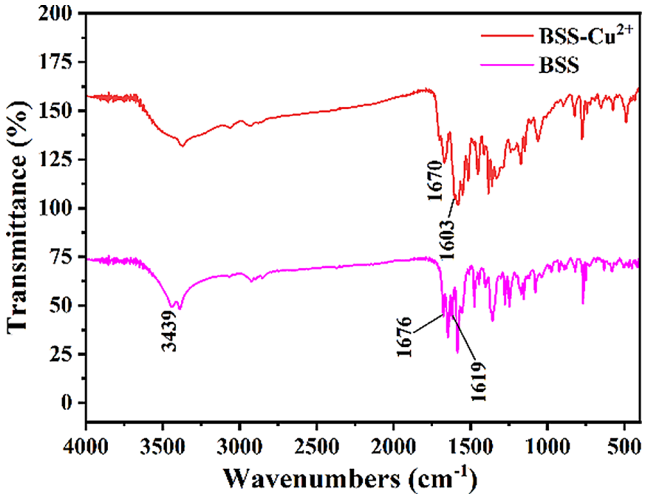

Fig. 5 Infrared spectra of probe BSS and complex BSS-Cu^{2+}

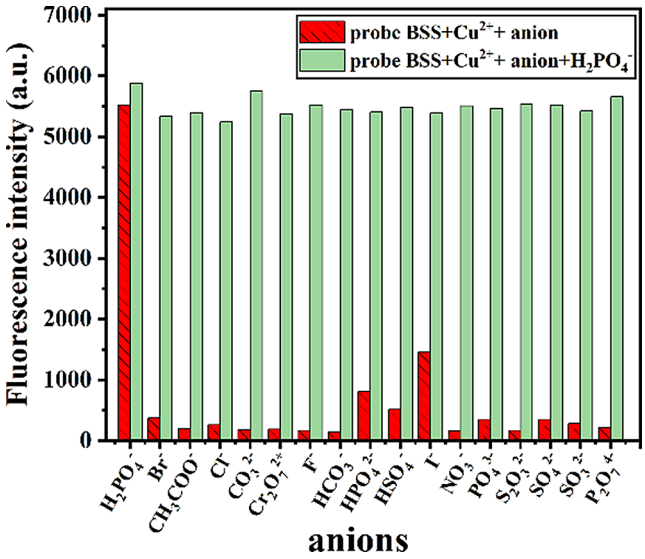

Fig. 7 Effect of coexisting anions on the detection of $H_2PO_4^-$ by BSS-Cu^{2+} (10 μmol/L)

response time than other probes [23, 26, 27, 30, 31], which providing the advantage of immediate response to Cu^{2+} and $H_2PO_4^-$.

Application of Probe BSS

Tap water and Songhua River water were selected to investigate the performance of complex BSS-Cu^{2+} for the detection of $H_2PO_4^-$. As shown in Table 1, the recoveries of $H_2PO_4^-$ in actual water samples were in the range of 99.00%~101.62% with the relative standard deviations (RSD) of 0.17%~3.22%, which indicated that complex BSS-Cu^{2+} had good accuracy and stability for $H_2PO_4^-$detection of in actual water samples.

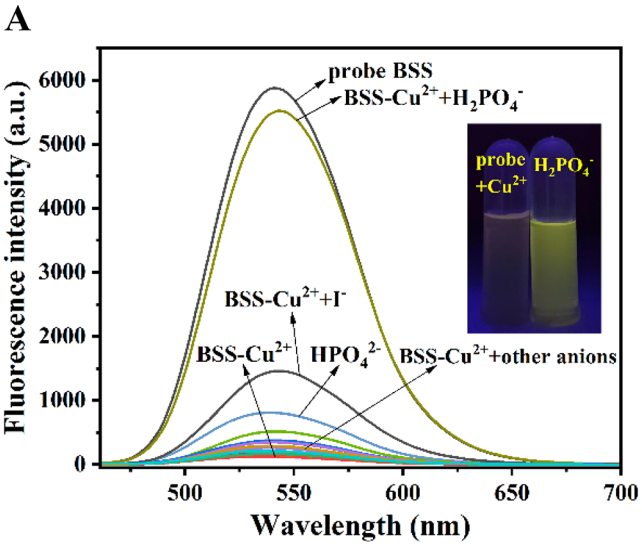

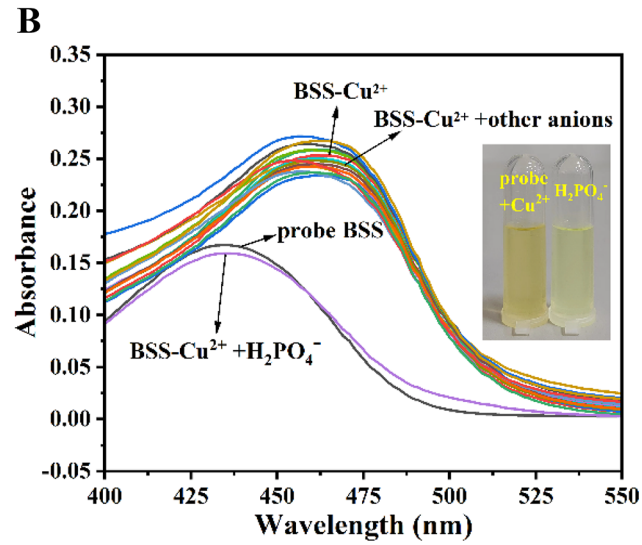

Fig. 6 (**a**) Fluorescence spectra of complex BSS-Cu^{2+} (10 μmol/L) with different anions. Inset in **a** showed fluorescence change of BSS-Cu^{2+} with $H_2PO_4^-$ under 365 nm. (**b**) UV spectrum of complex BSS-Cu^{2+} (10 μmol/L) with different anions. Inset in **b** showed color change of BSS-Cu^{2+} with $H_2PO_4^-$ under the sun lamp

Conclusions

In this paper, a Schiff base fluorescent probe BSS, which take naphthylimide as a fluorescent group and carbonyl, hydroxyl, imine groups as recognition groups was designed and synthesized. BSS could achieve "ON-OFF-ON" sequential fluorescence detection of Cu^{2+} and $H_2PO_4^-$ in acetonitrile solution, and detection process with advantages of short time (6 s), good selectivity, strong immunity to interference, large Stoke's shift, and visualization. BSS had favorable sensitivity with detection limits as low as 7.0×10^{-8} mol/L and 5.7×10^{-8} mol/L for Cu^{2+} and $H_2PO_4^-$ respectively. Complex BSS-Cu^{2+} could realize $H_2PO_4^-$ detection

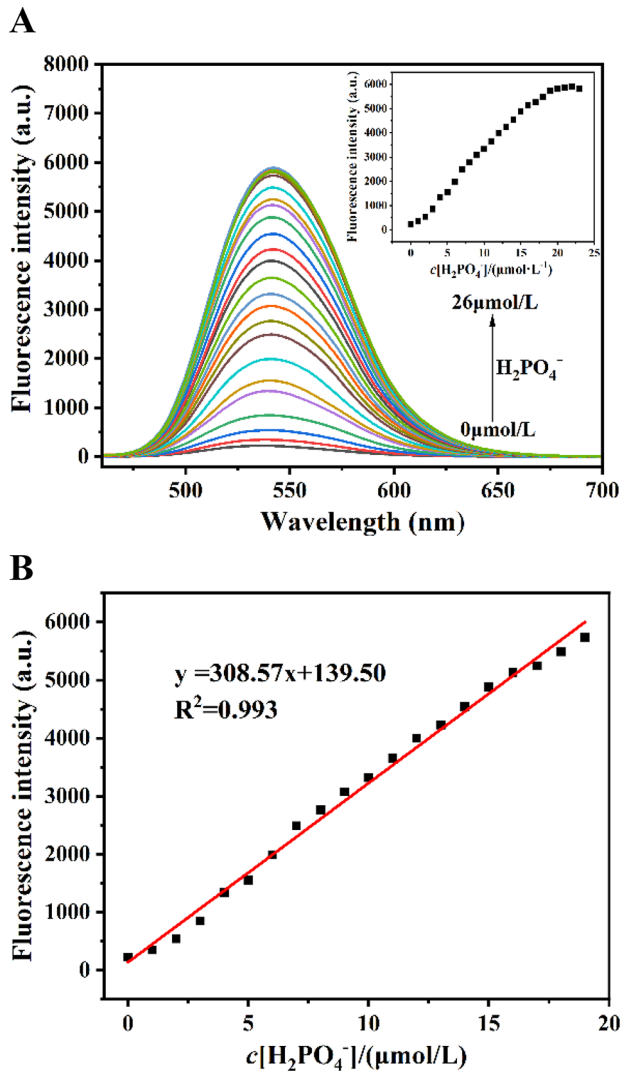

Fig. 8 (**a**) Fluorescence spectra and titration curves (as Inset showed) of BSS-Cu^{2+} at different $H_2PO_4^-$concentrations (0–26 μM). (**b**) Linear relationship between fluorescence intensity at 541 nm and $H_2PO_4^-$ concentration(0–19 μM)

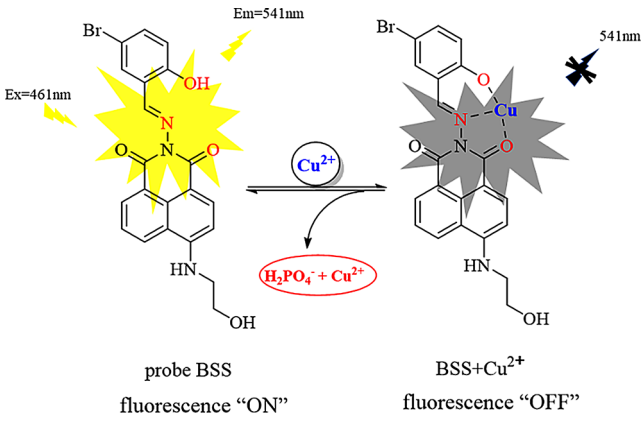

Fig. 10 Possible mechanism for continuous recognition of Cu^{2+} and $H_2PO_4^-$ by probe BSS

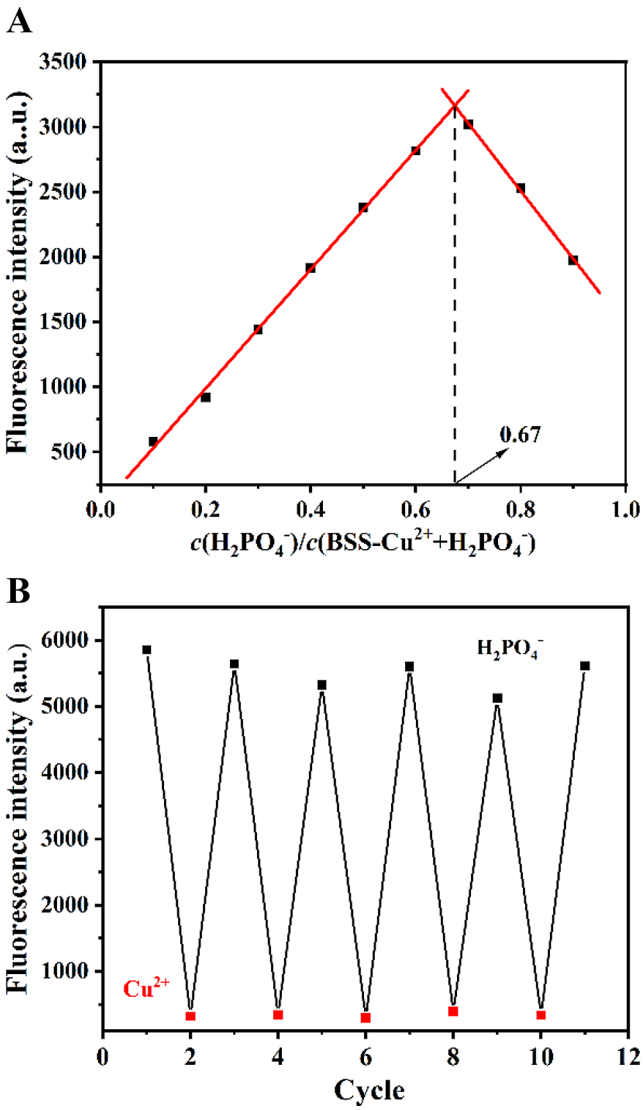

Fig. 9 (**a**) Job's plot of BSS-Cu^{2+} with $H_2PO_4^-$, in which c(BSS-Cu^{2+}+$H_2PO_4^-$)=10 μmol/L. (**b**) Reversibility experiments with alternate addition of Cu^{2+} and $H_2PO_4^-$ to probe BSS (10 μmol/L)

in water with recoveries of 99.00%~101.62% and RSD of 0.17%~3.22%, which provide a new detection of $H_2PO_4^-$ in the environmental field.

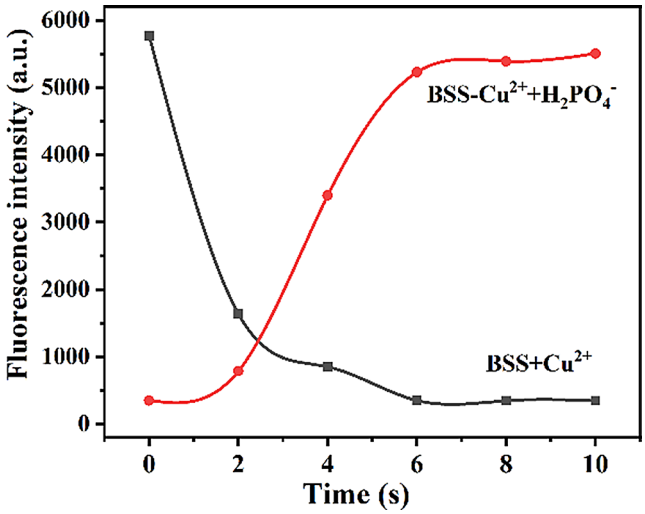

Fig. 11 Response time plots of probe BSS as well as BSS-Cu^{2+} to Cu^{2+} and $H_2PO_4^-$

Table 1 Determination of $H_2PO_4^-$ in actual water samples

Sample	Added/(μM)	Found/(μM)	Recovery rate/%	RSD/% ($n=3$)
Songhua River water	4.00	3.99	99.75	3.22
	8.00	8.13	101.62	0.17
	12.00	11.88	99.00	0.55
	16.00	15.98	99.88	1.35
Tap water	4.00	4.01	100.25	1.06
	8.00	7.94	99.25	1.64
	12.00	12.01	100.08	0.23
	16.00	15.87	99.19	0.84

Supplementary Information The online version contains supplementary material available at https://doi.org/10.1007/s10895-024-03692-y.

Acknowledgements The authors express appreciation to the School of Materials Science and Chemical Engineering, Harbin University of Science and Technology and Institute of Petrochemistry Heilongjiang Academy of Sciences for supporting this investigation. The authors would like to thank the anonymous reviewers and he editors.

Author Contributions Shukui Pang: Conceptualization, Methodology, Investigation, Visualization, Formal analysis, Writing – original draft. Yanchao Yu & Mianyuan Wu: Conceptualization, Methodology, Resources, Writing – review & editing, Supervision. Panru Zu & Canyao Wu: Software, Investigation, Formal analysis. Wenju Wu: Writing – review & editing. Jun You: Conceptualization, Methodology, Resources, Writing – review & editing, Supervision.

Funding This work was supported by National Science Foundation of China (22278098, 22008045) and Natural Science Foundation of Heilongjiang Province (No. LH2021H001, LH2023B013).

Data Availability All data generated or analyzed during this study are included in this published article and its supplementary information files.

Declarations

Ethics Approval This is an observational study. The Harbin University of Science and Technology has confirmed that no ethical approval is required.

Consent for Participate Not applicable.

Competing Interests The authors declare no competing interests.

References

1. Pecorino L (2021) Molecular biology of cancer: mechanisms, targets, and therapeutics. Oxford University Press
2. Brady D, Crowe M, Turski M et al (2014) Copper is required for oncogenic BRAF signalling and tumorigenesis. Nature 509:492–496
3. Chen J, Jiang Y, Shi H et al (2020) The molecular mechanisms of copper metabolism and its roles in human diseases. Pflügers Archiv-European J Physiol 472:1415–1429
4. Fasae KD, Abolaji AO, Faloye TR et al (2021) Metallobiology and therapeutic chelation of biometals (copper, zinc and iron) in Alzheimer's disease: limitations, and current and future perspectives. J Trace Elem Med Biol 67:126779
5. Cotruvo JA Jr., Aron AT, Ramos-Torres KM, Chang, Christopher J (2015) Synthetic fluorescent probes for studying copper in biological systems. Chem Soc Rev 44(13):4400–4414
6. Hinge SP, Orpe MS, Sathe KV et al (2016) Com-bined removal of rhodamine B and thodamine 6G from wastewater using novel treatment approaches based on ultrasonic and ultraviolet irradiations. Desalin Water Treat 57:1–13
7. Hu N-W, Yu H-W, Deng B-L et al (2023) Levels of heavy metal in soil and vegetable and associated health risk in peri-urban areas across China. Ecotoxicol Environ Saf 259:115037
8. Chen H, Teng Y, Lu S et al (2015) Contamination features and health risk of soil heavy metals in China. Sci Total Environ 512:143–153
9. Zhao M, Wang R, Yang K et al (2023) Nucleic acid nanoassembly-enhanced RNA therapeutics and diagnosis. Acta Pharm Sinica B 13(3):916–941
10. Wu X, Gilchrist AM, Gale PA (2020) Prospects and challenges in anion recognition and transport. Chem 6(6):1296–1309
11. Katayev EA, Sessler JL, Ustynyuk YA (2009) New strategy and methods for constructing artificial macrocyclic anion receptors. Selective binding of tetrahedral oxoanions. Russ Chem Bull 58:1785–1798
12. Vervloet MG, van Ballegooijen AJ (2018) Prevention and treatment of hyperphosphatemia in chronic kidney disease. Kidney Int 93(5):1060–1072
13. Sun S, Jiang K, Qian S-H (2017) Applying carbon dots-metal ions ensembles as a multichannel fluorescent sensor array: detection and discrimination of phosphate anions. Anal Chem 89:5542–5548
14. Yin H-B, Keng M (2014) Simultaneous removal of ammonium and phosphate from eutrophic waters using natural calci-um-rich attapulgite-based rersatile adsorbent.Desali-nation. 351:128–137
15. Kundu S, Coumar MV, Rajendiran S et al (2015) Phosphates from detergents and eutrophication of surface water ecosystem in India. Curr Sci 1320–1325
16. Sun C, Wang S, Wang H et al (2022) Internal nitrogen and phosphorus loading in a seasonally stratified reservoir: implications for eutrophication management of deep-water ecosystems. J Environ Manage 319:115681

17. Chen Z, Fang F, Shao Y et al (2021) The biotransformation of soil phosphorus in the water level fluctuation zone could increase eutrophication in reservoirs. Sci Total Environ 763:142976
18. Katano H, Ueda T (2011) Spectrophotometric determination of phosphate anion based on the formation of molybdophosphate in ethylene glycol-water mixed solution. Anal Sci 27:1043–1047
19. Karthikeyan R, Berchmans S (2013) Inorganic-organic composite matrix for the enzymatic detection of phosphate in food samples. J Electrochem Soc 160:73–77
20. Udnan Y, McKelvie ID, Grace MR (2005) Evaluation of on-line preconcentration and flow-injection amperometry for phosphate determination in fresh and marine waters. Talanta 66:461–466
21. Ding Q, Li C, Wang H et al (2021) Electrochemical detection of heavy metal ions in water. Chem Commun 57(59):7215–7231
22. Chudobova D, Dostalova S, Ruttkay-Nedecky B et al (2015) The effect of metal ions on Staphylococcus aureus revealed by biochemical and mass spectrometric analyses. Microbiol Res 170:147–156
23. Ahmed N, Zareen W, Zhang D et al (2022) Irreversible coumarin based fluorescent probe for selective detection of Cu^{2+} in living cells. Spectrochim Acta Part A Mol Biomol Spectrosc 264:120313
24. Chen W, Liang H, Wen X et al (2022) Synchronous colorimetric determination of CN, F, and H_2PO_4 based on structural manipulation of hydrazone sensors. Inorg Chim Acta 532:120760
25. Luo C, Zhang Q, Sun S et al (2023) Research progress of auxiliary groups in improving the performance of fluorescent probes. Chemical Communications
26. Yao G, Fang S, Yin P et al (2023) A colorimetric and fluorometric dual-mode probe for Cu^{2+} detection based on functionalized silver nanoparticles. Environ Sci Pollut Res 1–9
27. Xiong J, Li Z, Tan J et al (2018) Two new quinoline-based regenerable fluorescent probes with AIE characteristics for selective recognition of Cu^{2+} in aqueous solution and test strips. Analyst 143(20):4870–4886
28. Meng X, Li S, Ma W et al (2018) Highly sensitive and selective chemosensor for Cu^{2+} and H_2PO_4 based on coumarin fluorophore. Dyes Pigm 154:194–198
29. Arabahmadi R (2022) Antipyrine-based Schiff base as fluorogenic chemosensor for recognition of Zn^{2+}, Cu^{2+} and H_2PO_4 in aqueous media by comparator, half subtractor and integrated logic circuits. J Photochem Photobiol A 426:113762
30. La Y-T, Yan Y-J, Gan L-L et al (2023) A fluorescent salamo-salen-Salamo-Zn (II) sensor for bioimaging and biosensing H_2PO_4 in zebrafish and plants. Spectrochim Acta Part A Mol Biomol Spectrosc 303:123159
31. Zhao L, Chen K, Xie K et al (2023) A benzothiazole-based on-off fluorescence probe for the specific detection of Cu^{2+} and its application in solution and living cells. Dyes Pigm 210:110943
32. Zhu H, Liu C, Su M et al (2021) Recent advances in 4-hydroxy-1, 8-naphthalimide-based small-molecule fluorescent probes. Coord Chem Rev 448:214153
33. Xie Z-D, Fu M-L, Yin B, Zhu Q (2018) Research Progress in 1, 8-Naphthalimide-based fluorescent probes for two-photon imaging. Chin J Org Chem 38(6):1364–1376
34. Han C, Sun S-B, Ji X et al (2023) Recent advances in 1,8-naphthalimide-based responsive small-molecule fluorescent probes with a modified C4 position for the detection of biomolecules. TRAC Trends Anal Chem 117242
35. Liu Q, Li S, Wang Y et al (2023) Sensitive fluorescence assay for the detection of glyphosate with $NACCu^{2+}$ complex. Sci Total Environ 882:163548
36. Jang H-J, Jo T-G, Kim C (2017) A single colorimetric sensor for multiple targets: the sequential detection of Co^{2+} and cyanide and the selective detection of Cu^{2+} in aqueous solution. RSC Adv 7(29):17650–17659